

## ISRU Pilot Excavator Wheel Testing in Lunar Regolith Simulant

Liz Zhang,<sup>1</sup> Jason Schuler,<sup>2</sup> Adam Dokos,<sup>3</sup> Yinan Xu,<sup>4</sup> Evan Bell,<sup>5</sup> Thomas Muller<sup>6</sup>

<sup>1</sup>University of Illinois Urbana-Champaign; email: [elz2@illinois.edu](mailto:elz2@illinois.edu)

<sup>2</sup>NASA Kennedy Space Center, FL; email: [jason.m.schuler@nasa.gov](mailto:jason.m.schuler@nasa.gov)

<sup>3</sup>NASA, Kennedy Space Center, FL; email: [adam.g.dokos@nasa.gov](mailto:adam.g.dokos@nasa.gov)

<sup>4</sup>University of Arizona; email: [yinanx@arizona.edu](mailto:yinanx@arizona.edu)

<sup>5</sup>NASA, Kennedy Space Center, FL; email: [evan.a.bell@nasa.gov](mailto:evan.a.bell@nasa.gov)

<sup>6</sup>Bennett Aerospace, Kennedy Space Center, FL; email: [thomas.j.muller@nasa.gov](mailto:thomas.j.muller@nasa.gov)

### ABSTRACT

The ISRU Pilot Excavator, or IPEX, is a robotic excavator funded by NASA's Space Technology Mission Directorate (STMD). The Concept of Operations for IPEX involves the robot driving on the lunar surface up to 70 km at a speed of up to 30 cm/s. As such, it is critical to the mission's success to optimize the design of the wheels for performance in lunar conditions, specifically in lunar regolith. To achieve this, an array of tests was completed to observe the effects of various wheel design choices on the driving performance of the wheels in lunar regolith simulant.

In order to facilitate testing, we designed a 12" dia. configurable wheel to allow for interchangeability between various wheel formations. Two types of wheel parts were designed to be swapped: cleats, which form the tread of the wheel; and grousers, which protrude from the treads. The test variables that we considered were as follows: square vs. round wheel shape, solid vs. perforated cleats, cleat spacing, grouser height, and grouser spacing. By combining different settings of each of these test variables, ten discrete wheel designs were created and tested.

The configurable test wheels were mounted on the Regolith Advanced Surface Systems Operations Robot (RASSOR) developed at NASA's Kennedy Space Center. In our experiments, the robot was driven at a controlled speed across a prepared surface of BP-1 lunar regolith simulant. Four types of tests were conducted: circle driving, straight driving, slope driving, and drawbar pull. The driving tests were chosen to mimic a variety of conditions in which IPEX may be expected to operate, and the drawbar pull test was chosen to provide a standard of comparison with existing wheel design literature. The circle and straight driving tests were each performed at different levels: for the circle driving test, the robot was driven at a constant linear speed and three different angular speeds, while for the straight driving test, the robot was driven at three different linear speeds. The data collected from these tests included the power usage from each of the wheels, measurements of the tread patterns left in the regolith surface, and the amount of slip the wheels experienced, which was calculated using data from an OptiTrack motion capture system.

From the results of these experiments, we found that certain test variables were more significant than others in determining performance for each type of test, and no single wheel design clearly outperformed the others in all areas. The details of our findings will be discussed further in this paper. This data will be utilized to inform the design of the wheels for IPEX and can provide a basis for the design of wheels for future lunar terrain vehicles.

## **INTRODUCTION**

The In-Situ Resource Utilization (ISRU) Pilot Excavator (IPEX) Project will develop a 30 kg-class excavator to demonstrate robotic excavation of up to 10 metric tons of lunar regolith (Schuler et al. (2022)). This is an evolution of RASSOR 2.0 (Mueller et al. (2016)) and is volumetrically scaled between 50-70% of RASSOR 2.0. The overall structures of RASSOR 2.0 and IPEX are similar, with both robots being comprised of a chassis, 4 wheels, and two arms with bucket drums attached to the ends. They also both utilize a form of steering called “skid-steer”, where the wheels on the left and right sides of the robot are each synced with each other and both sides are controlled independently. In skid-steer, the wheels do not pivot relative to the chassis, and the robot instead turns by running the left and right wheels at different speeds. By utilizing skid-steer, IPEX differs significantly from previous NASA rovers.

Over the course of its mission, IPEX will be expected to drive upwards of 70 km on the lunar surface at speeds of up to 30 cm/s in order to excavate regolith. This driving distance and speed are unique compared to other extraterrestrial rovers. Additionally, full-scale sustained ISRU efforts, as are expected within the next decade, will require excavation of thousands of tons of regolith per year. This will further increase the expected driving time for IPEX-like excavation rovers. Since driving constitutes a large portion of IPEX’s mission and energy costs, we found it essential to optimize the design of the IPEX wheels for the best performance in lunar regolith. This necessitated testing of the performance of several different wheel designs in lunar regolith simulant, specifically focusing on driving efficiency and energy usage.

While there is an abundance of existing literature about the design of wheels for extraterrestrial rovers in regolith simulant, such as Ding et al. (2011) and Nagaoka et al. (2020), our research was unique for several reasons. First, our testing was conducted using RASSOR 2.0, a fully developed robot, as a test platform. Since RASSOR 2.0 and IPEX have very similar designs, this allowed us to simulate IPEX with high fidelity. Additionally, since RASSOR 2.0 also utilizes skid-steer similarly to IPEX, this research constitutes a novel exploration of the efficacy of skid-steering for extraterrestrial rovers. Finally, testing was conducted in the KSC Regolith Test Bed (RTB), which contains 120 tons of BP-1 lunar simulant with a volume of 8m x 8m x 1.1m. This allowed us to observe wheel performance while continuously driving the robot distances of over 8m, which was much larger than previously tested in existing literature.

The primary goal of this work is to compare the performance of several wheel designs with various design factors to understand how those wheel design factors affect the slip and power usage of the wheels in a variety of driving conditions. This research will be used to inform the design of IPEX’s wheels.

## **EXPERIMENTAL VARIABLES**

### **Wheel Configurations:**

The test wheels were designed to be fully reconfigurable with the capability of easily swapping the cleats and grousers. Grousers are used to increase wheel traction and thought to provide the greatest effect on wheel thrust. We included two types of grouser designs: curved and square. Each type of grouser was developed at three different heights, named from shortest to longest as flat, short, and tall. Since the rover utilizes skid-steer for maneuvering, which is different than every interplanetary rover to date, understanding the effect of changing the geometrical shape is a critical part of this study. Testing multiple grouser configurations will provide data to compare

relationships between different grouser heights, shapes, and spacings to better understand their impact on different types of motion, such as turning and driving in a straight line. Cleats follow the same design concept, also incorporating two shape options: curved and square. From testing with RASSOR 2.0 (Mueller et al. (2016)), it was observed that a curved cleat prevents wheels from digging into the regolith during skid-steer turning. In addition to the curved and square features, cleats are designed with both “solid” and “with holes” configurations. The cleat configurations were chosen to better understand the effect of soil compaction between the grousers and provide data on the effects of adding holes for mass reduction. Examples of different combinations of cleats and grousers are shown in Figure 1. The overall design of the configurable wheel was informed by Lawton (2020).

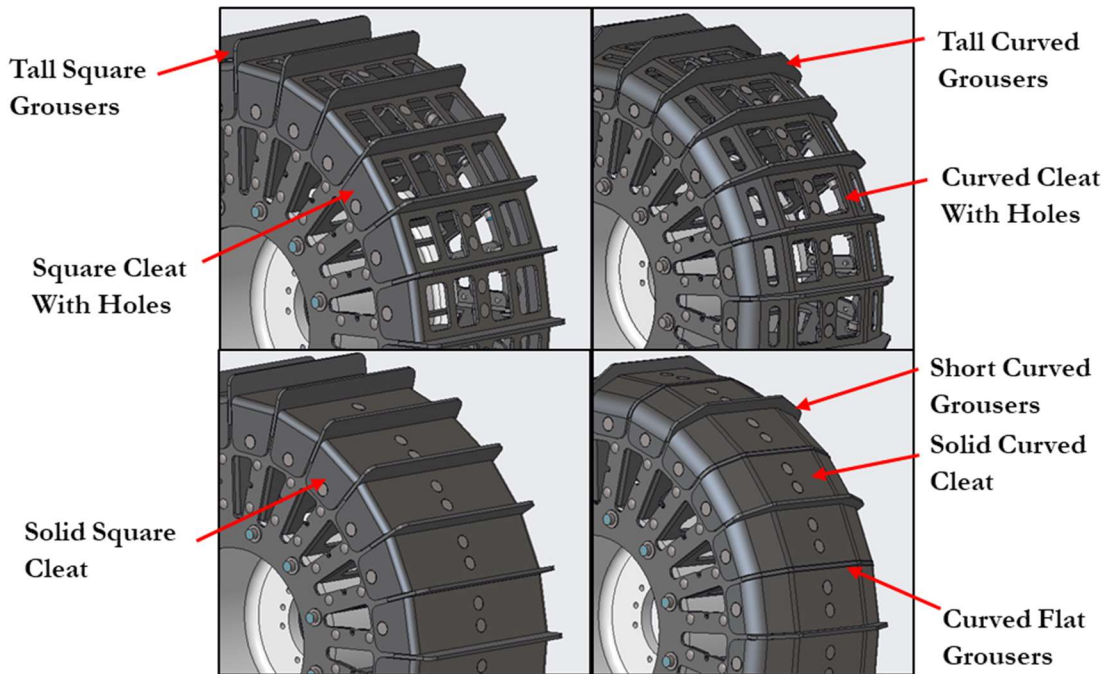


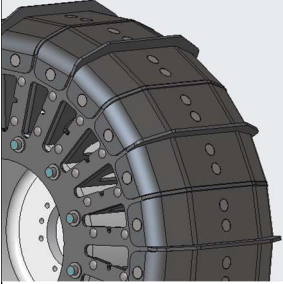
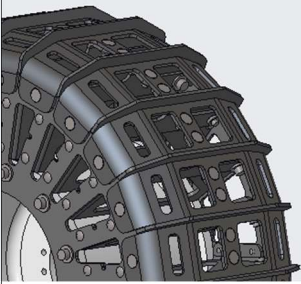
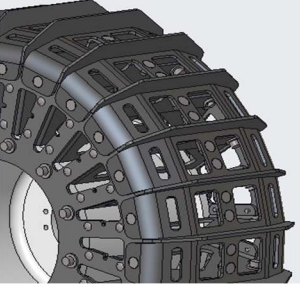
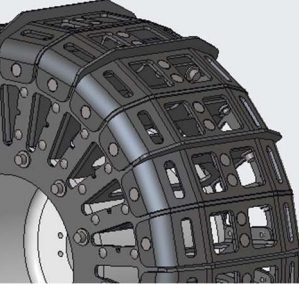
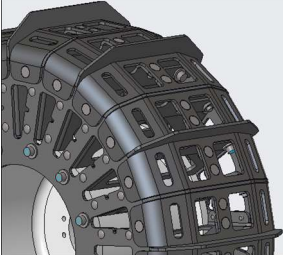
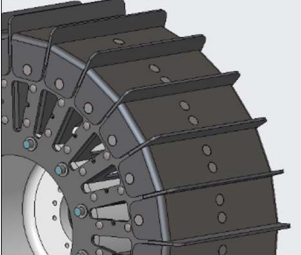
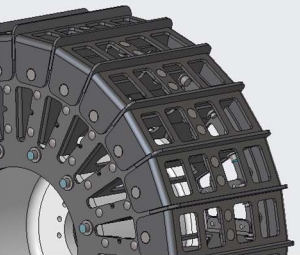
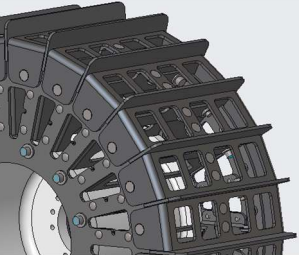
**Figure 1. Four wheel configurations with descriptions of cleat and grouser designs.**

In the context of this study, a total of four sets of cleats and six sets of grousers were designed, resulting in a comprehensive set of 24 unique configurations. However, to optimize research within the constraints of time and resources, a selection process was used to refine our experimental focus. This process prioritized configurations considered to offer the highest utility. Consequently, ten distinct wheel configurations were selected for testing, as shown in Table 1; 5a and 6a each represent the removal of every other cleat on the wheel.

### **Test Types:**

We conducted four different types of tests: circle driving, straight line driving, slope driving, and drawbar pull. The three driving tests were chosen to simulate expected driving conditions for different parts of IPEX’s mission, while the drawbar pull test was chosen as a standard of comparison to existing wheel testing literature (Creager 2017). For the circle and straight line driving tests, we commanded the robot to drive using combinations of angular and linear speeds which increased incrementally (see Table 2). Since RASSOR 2.0 uses skid-steer, these speeds translated to rotational speeds of the wheels using the following two equations:

**Table 1. Wheel Testing Configurations**

			
<b>Test 3: Curved Solid Cleat + Curved Short Grousers and Curved Flat Grousers</b>	<b>Test 5/5a: Curved holes Cleat + Curved Short Grousers</b>	<b>Test 6/6a: Curved holes Cleat + Curved Tall Grousers</b>	<b>Test 7: Curved holes Cleat + Curved Short Grousers and Curved Flat Grousers</b>
			
<b>Test 8: Curved holes Cleat + Curved Tall Grousers and Curved Flat Grousers</b>	<b>Test 10: Square Solid Cleat + Square Tall Grousers</b>	<b>Test 13: Square Holes Cleat + Square Short Grousers</b>	<b>Test 14: Square Holes Cleat + Square Tall Grousers</b>

**Equation 1. Left and Right Wheel Velocity for Skid-Steer Robot**

$$V_{\text{left}} = (x - z*b)/(2*r)$$

$$V_{\text{right}} = (x+z*b)/(2*r)$$

Where  $x$  = linear speed (m/s),  $z$  = length of robot's wheelbase (0.5207 m),  $b$  = angular speed (rad/s), and  $r$  = wheel radius (0.1524 m).

We chose the speeds in Table 2 based on the expected driving conditions for IPEX. For instance, since IPEX's nominal maximum speed is 0.3 m/s, this was also the maximum speed we tested.

For the slope test, we commanded the robot to drive up a prepared slope of BP-1 simulant with an inclination of  $20^\circ$  ( $\pm 0.5^\circ$ ) and a length of 1 m. This angle was chosen based on the nominal slope IPEX is expected to be able to traverse. For the drawbar pull test, we attached a sled to the

back of the robot and commanded it to drive at a constant speed while incrementally adding weights to the sled as it drove.

**Table 2. Linear and Angular Speeds by Test Type**

Test Type	Linear Speed (m/s)	Angular Speed (rad/s)
Circle 1	0.20	0.35
Circle 2	0.20	0.30
Circle 3	0.20	0.20
Line 1	0.10	0.00
Line 2	0.20	0.00
Line 3	0.30	0.00
Slope	0.20	0.00
Drawbar Pull	0.10	0.00

Due to time constraints, we did not test all ten wheel configurations with all four test types; after conducting circle and straight line driving tests for all wheel configurations, we analyzed the data and chose a few wheel configurations to conduct slope tests, then narrowed down our selection once again for the drawbar pull test. In total, we conducted 83 tests (see Table 3).

**Table 3. Final Test Matrix**

Test Type	Wheel Configurations Tested	Trials Per Configuration
Circle	3, 5, 5a, 6, 6a, 7, 8, 10, 13, 14	3
Line	3, 5, 5a, 6, 6a, 7, 8, 10, 13, 14	3
Slope	5, 5a, 6, 6a, 13	3
Drawbar Pull	5, 6	4

## EXPERIMENTAL SETUP

Tests were conducted using the Regolith Advanced Surface Systems Operations Robot (RASSOR) 2.0 as a test platform. RASSOR 2.0, like IPEX, is comprised of a chassis with 4 wheels and an arm with bucket drum excavation tools attached to the front and back. It also utilizes skid-steering. Because of the closeness in design and controls between RASSOR 2.0 and IPEX, it was an ideal platform to use for testing. The crucial distinction was the difference in size; IPEX is a 30 kg class excavator while RASSOR 2.0 is approximately 66 kg. We decided to use IPEX-sized wheels, which were 30.5 cm in diameter, and mount them to RASSOR 2.0 in place of its own 43 cm dia. wheels. This meant that there was much more weight applied to the

test wheels than we would reasonably expect them to experience on IPEX in a lunar environment. However, we did not feel that this weight difference would cause a significant difference in the impact of the wheel design factors we were testing. Since our tests primarily focused on comparing various wheel design factors rather than exactly reproducing the conditions that IPEX would experience, we felt that using RASSOR 2.0 with its current weight was adequate for our needs. Future tests will be performed on a lunar weight IPEX platform.

To simulate the lunar surface, we used BP-1 (Black Point 1) lunar simulant in KSC's RTB. BP-1, from Schuler et al. 2022, is "an inexpensive geotechnical lunar regolith simulant sometimes used for excavation and mobility testing". BP-1 is derived from basalt, simulating lunar mare soils, and its granular size distribution falls within one standard deviation of the actual lunar regolith particle distribution returned by Apollo lunar missions. Since the geotechnical properties of BP-1 can vary significantly based on environmental and internal factors, it was critical for us to develop and maintain a rigorous procedure for preparing the RTB between tests. Details of the test bed preparation can be found in the Test Procedure below. Inside of the RTB, we utilized a motion capture system from OptiTrack to accurately and precisely track RASSOR 2.0's location as it drove within the test area. This was done using six OptiTrack cameras mounted at specific locations on the walls of the RTB and an IR marker attached to RASSOR 2.0's chassis. Through this OptiTrack system, we were able to log the robot's position and movements with positional error of less than 0.3 mm.

A useful advantage of using RASSOR 2.0 as our test platform was that it was already equipped to collect most of the data we needed. Data was logged through Robot Operating System (ROS) at approximately 20 Hz. During each test, we collected the following data from ROS while driving the robot:

- Distance traveled (according to the OptiTrack system)
- Distance the robot was commanded to travel
- Current draw from the motors in each wheel
- Battery pack voltage
- Time
- Force data from a load cell (only used during drawbar pull test)

The load cell was connected to the straps of the sled for the drawbar pull test (see Figure 7) in order to collect data on the amount of drawbar pull force that the robot was able to exert. To do this, we used an Interface force transducer (model SM-250) which logged at a rate of 100 Hz. This sensor has a measuring range of  $\pm 150$  lbf and a nonlinearity of  $\pm 0.03\%$  of full-scale output.

## **TEST PROCEDURE**

### **Test Bed Preparation:**

The BP-1 test bed was carefully prepared between each test to ensure repeatability and consistency across tests. This preparation involved three major steps: leveling, compacting, and raking. These steps were taken to create a test surface which would be uniform and create a mix of conditions to simulate a variety of conditions on the lunar surface.

First, the test bed was leveled using several tools, such as an 80-20 beam and a wide rake, to spread BP-1 evenly. This step was especially essential because the robot's driving created indents in the test surface that needed to be filled in order to maintain uniformity. The levelness of the surface was evaluated every 2 feet in both the X and Y directions on the prepared surface using a

24" bubble level. For the slope test, the inclined surface was evaluated using a digital inclinometer attached to a 40" 80-20 beam. The angle of incline was prepared to be  $20^\circ \pm 0.5^\circ$ . Next, the leveled area was compacted using a 50-lb weight placed in the center of a plastic bin. This was dragged across the surface of the regolith in a crosshatch pattern with a 50% overlap between passes, as shown in Figure 2. While compacting, care was taken to ensure that the bin was dragged parallel to the surface to avoid upturning the regolith as much as possible. The compaction was tested using hand geotechnical tools, such as a Humboldt Soil Penetrometer, at several random locations to ensure consistency. After compacting, the bulk density of the BP-1 was approximately  $1.75 \text{ g/cm}^3$ , with a margin of error of less than 5%.



**Figure 2. A team member using the bin-and-weight compaction method in a crosshatch pattern.**

Finally, the test bed was fluffed using a wide rake making passes in a crosshatch pattern with 50% overlap. This was done in such a way to create an approximately 2.5 cm layer of low-density regolith on top of the compacted regolith. The final appearance of the prepared test bed can be seen in Figure 3.



**Figure 3. RASSOR 2.0 positioned on the prepared regolith test bed.**

### **Wheel Testing:**

While each type of test we conducted had its own individual differences, they each followed the same basic procedure. Before starting the test, the robot was manually positioned in the test bed so that all four wheels rested completely on the prepared surface. The robot's arms were positioned at a  $45^\circ$  angle above their horizontal position (see Figure 4), and the bucket drums were confirmed to be empty. To begin the test, we first began logging data through ROS, then sent a control command to run the robot at a constant linear/angular speed (as defined in Table 2) for each test. During the test, we closely observed the robot to notice any anomalies. Once the robot reached its final position for the test, we manually stopped it and halted our data logging.



**Figure 4. RASSOR 2.0 with its arms positioned at a 45° angle from the horizontal position.**

Each of the driving tests had a unique starting and stopping condition. For the circle test, we started the robot parallel near the edge of the RTB and stopped the test when the robot had approximately driven in a full circle, which occurred when it approached its initial position. For the straight line test, we initially positioned the robot on one end of the test bin and then stopped it when it was about to collide with the opposite wall of the test bin. This resulted in the robot traveling approximately 7.5m for each straight line test. For the slope test, we prepared a hole in the test bin with a 20° incline on one end (see Figure 5). The robot was initially positioned on the flat bottom section of the hole, and the test was stopped when all four of the robot's wheels had fully reached the top of the inclined surface.



**Figure 5. RASSOR 2.0 positioned at the bottom of the inclined surface before a slope test.**

The drawbar pull test was executed similarly to the straight line driving test, with the added component of a weighted sled. We affixed the sled to the robot by wrapping a strap around the back wheel hubs as shown in Figure 6, taking care to ensure the left and right sides were symmetrical. The robot was initially positioned such that both the wheels and the sled rested completely on the prepared test surface. We began with some initial weight on the sled, then after starting the robot, incrementally added weights of varying sizes to the sled. While adding weights, we attempted to keep the weight distribution as symmetrical as possible. We stopped the test when one of two conditions was met: either the wheels reached “full slip” (the robot was not moving forwards and instead the rotation of the wheels caused it to dig itself deeper in the regolith) or the robot reached the end of the test bed and could not continue.





**Figure 6. RASSOR 2.0 with a sled and attached load cell affixed to its back wheel hubs.**

Most of our data collection was automated through ROS, but we also collected other quantitative and qualitative data ourselves. During each of the slope and drawbar tests, we recorded videos of each trial to observe any differences in wheel performance and keep track of the timing of the test. For the drawbar pull test, in addition to the data from the load cell which was collected through ROS, we also recorded the amount and timing of the weight we added to the sled while the robot drove. After the circle and straight line tests, we photographed the tread patterns left over in the regolith for both the left and right wheels. For the slope and drawbar pull tests, since the wheel configurations we were testing were much more similar and the tread patterns did not show significant differences, we did not find it necessary to photograph them.

## RESULTS

While analyzing the data we collected during testing, we focused on comparing two metrics: slip rate and power consumption. We chose to study these metrics because we felt that they were the most important indicators of wheel performance for IPEX. Since IPEX is expected to traverse large distances with a limited amount of power, we wanted to find a wheel configuration that would allow it to travel the most efficiently, which depends on both wheel slip and power usage. While previous wheel testing literature has focused on slip, we felt that power usage was also an important factor to consider based on the concept of operations for IPEX and the relationship between skid-steering, slip, and power. We first examined slip and power individually, then combined the two metrics to find which wheel configuration performed the best overall. In addition, we also collected data from the load cell attached to the sled during the drawbar pull test, which we compared to the slip and power data from those tests.

### Wheel Slip

Slip was defined as the difference between the idealized distance we commanded the robot to travel (assuming a smooth 30.5 cm dia. wheel that perfectly rolled without slipping) and the actual distance it traveled, as measured using the OptiTrack motion capture system. Figure 7 shows an example graph of the cumulative slip over time for one of the driving test types. Since the goal for IPEX is to minimize the amount of slip that occurs, a wheel performs better when it accumulates the least amount of slip.

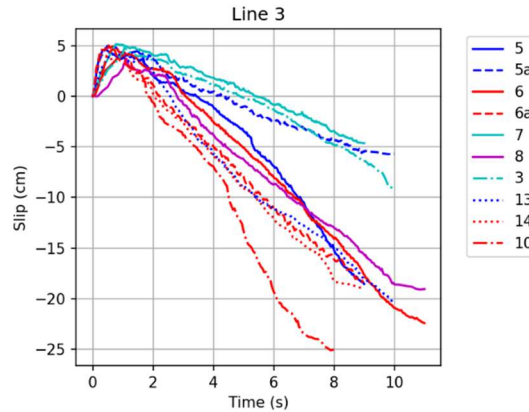


**Figure 7. Example graph of slip over time for a straight line driving tests**

In this graph, the blue lines represent wheel configurations with short grousers and the red lines represent wheel configurations with tall grousers. In general, the wheels with tall grousers tended to have less slip compared to the wheels with short grousers (with the exception of test wheel #5).

Since the trends we saw in the data appeared to be linear after about 2 seconds, we took a representative sample of the data (in the middle of the time range to allow for deviations due to acceleration and deceleration) and performed a linear regression to obtain a rate of slip over time, referred to as “slip rate”. The slip rate for each wheel configuration in each test is given in Figures 8-9. In Figures 8-12, the colors in each bar graph are related to the grouser design of each wheel configuration to allow for easier interpretation. The red bars (10 and 14) correspond to tall square grousers, the orange bars (13) correspond to short square grousers, the green bars (6, 6a, 8) correspond to tall round grousers, and the blue bars (3, 5, 5a, 7) correspond to short round grousers.

One interesting feature of our data was that in several instances, the slip and slip rate were negative, indicating that the tested wheel configuration performed better than the ideal wheel. We predict that this was caused by the added length of the grousers extending from the wheel, which could have increased the effective diameter of each wheel. However, since the goal of these experiments is to compare the wheel designs rather than to obtain objective values for slip and slip rate, we felt that our interpretation of the data was still valid.

We found that different wheel configurations performed differently based on the driving conditions. In general, the wheels with tall grousers (red and green bars on the graphs) tended to have a lower slip rate than the wheels with short grousers (orange and blue bars), and the wheels with square grousers (red and orange bars) tended to have a lower slip rate than the wheels with round grousers (green and blue bars), with the exception of wheel #5 in some cases. We did not note any significant differences between wheels using different cleat types. Additionally, due to loss of data, the results from the circle 2 test for wheel #3 will not be considered.

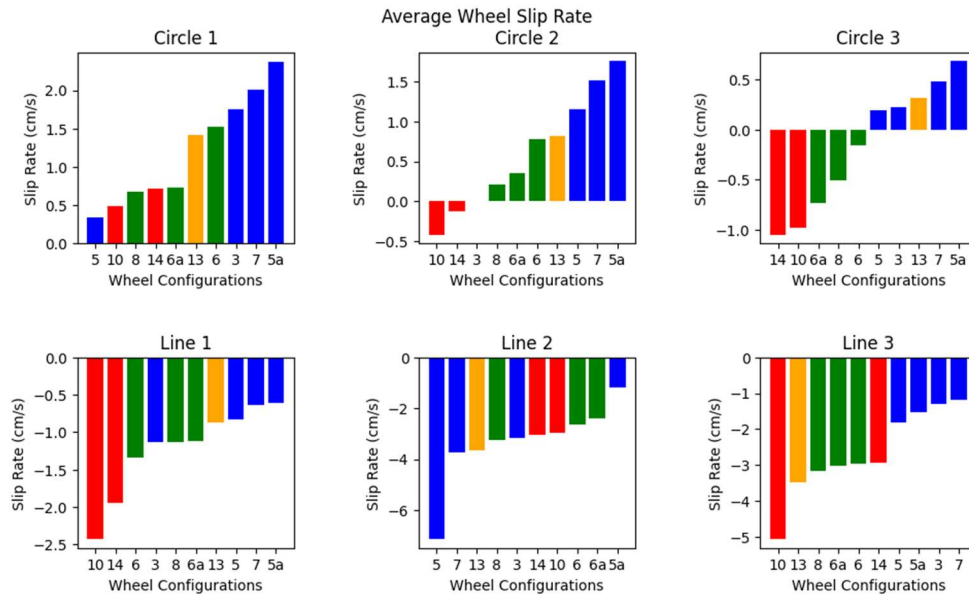


**Figure 8. Average wheel slip rate during circle and line tests, sorted from lowest to highest.**

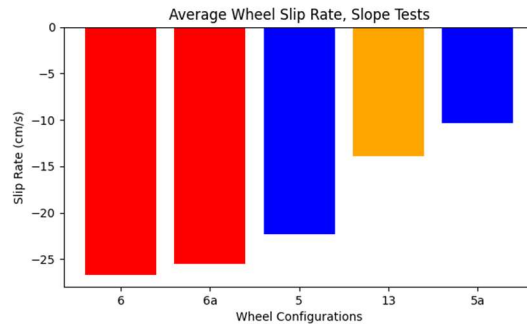


**Figure 9. Average wheel slip rate during slope driving tests, sorted from lowest to highest.**

### Power Usage:

To measure power, we used the current draw for each wheel motor multiplied by the applied voltage from the battery pack. We found that in most cases, there were not significant differences between the power usage of each wheel over time, so for each test, we took the average of the currents from each wheel and added them together, then multiplied this value by the average voltage of the battery pack to find a value for the average total power usage. These values can be seen in Figures 10 and 11 below. Our goal was to find which wheel designs used the least amount of power.

Once again, we found that while there were not significant differences between wheels with different cleat designs, there were significant differences in performance between wheels with different grouser designs. Here, we can observe the opposite trend from the wheel slip; wheels with tall grousers and wheels with square grousers had a higher power consumption than wheels with short and round grousers, respectively. The wheel with the best overall power consumption

seems to be wheel #3 for the circle driving tests and wheel #5a for the straight line driving tests, while the wheels that performed the worst overall were wheels #6/6a.

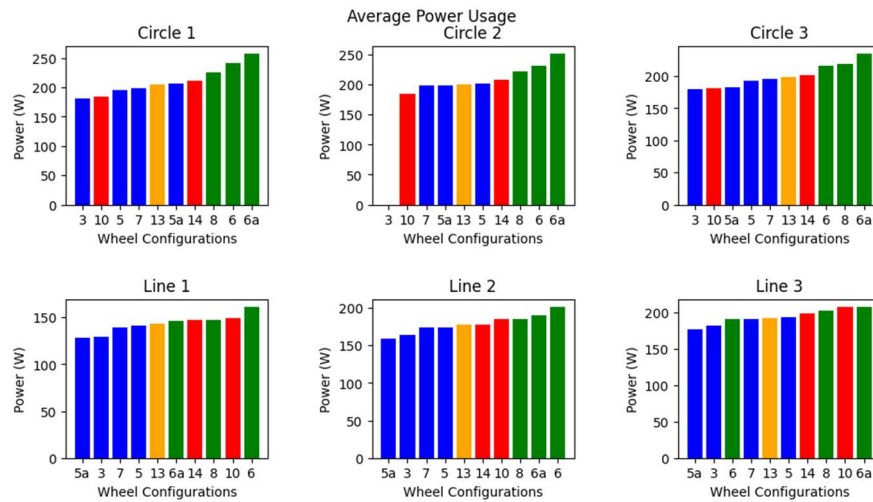


**Figure 10. Average power usage for all wheels during circle and line tests, sorted from lowest to highest.**

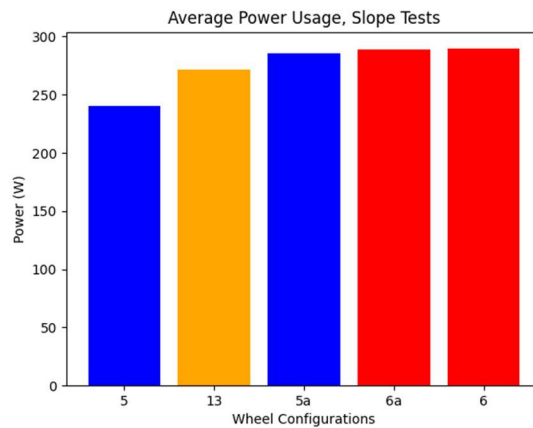


**Figure 11. Average power usage for all wheels during slope tests, sorted from lowest to highest.**

In addition to analyzing the total power usage of all 4 wheels while driving, we also analyzed the power usage from the left vs right wheels. This was especially relevant for the circle driving tests since the skid-steering system causes the left and right wheels to rotate at different speeds. Figure 12 shows the average power usage for the left vs right wheels during each circle test. When observing the power usage from the left and right wheels separately, the ordering of least to most power usage changes dramatically. The main difference is that the left wheels for the wheel configurations with round grousers seem to use less power. These round wheels may therefore be better suited for rovers utilizing skid-steer.

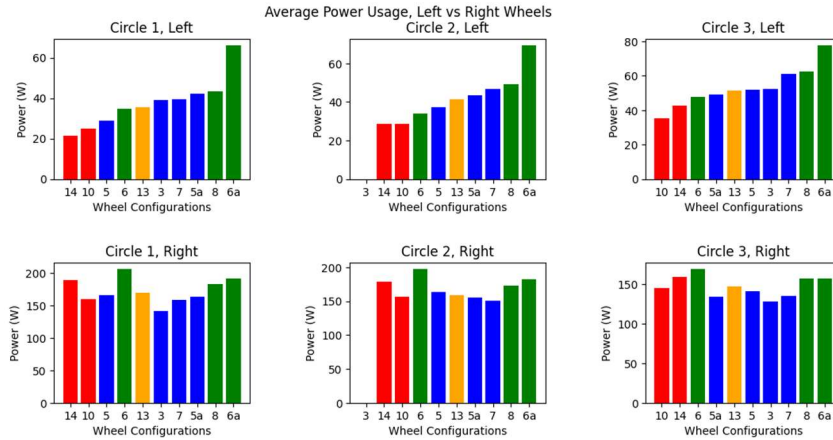


**Figure 12. Average power usage for left vs right wheels during circle tests, sorted from lowest to highest based on the left wheel.**

### Drawbar Pull Force:

While the drawbar pull force was not a metric we directly considered while analyzing wheel performance, this data still provided useful insight on the wheel design, especially in comparison to existing literature. From Figure 13, we can observe that wheel #6, which had tall grouser, had greater peak power consumption and was able to exert more force than wheel #5.

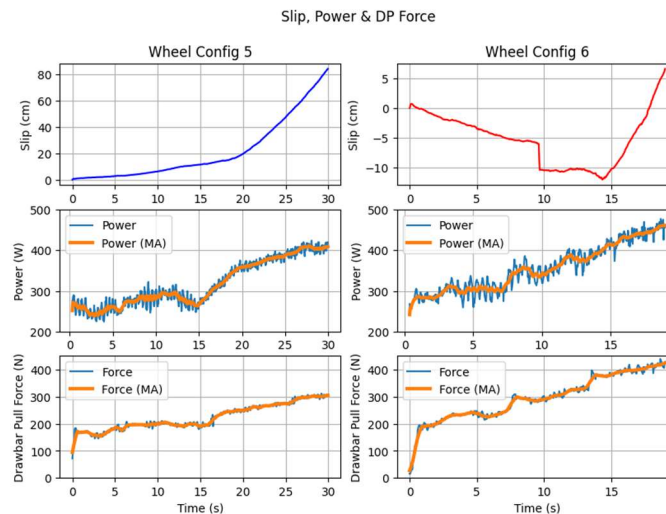


**Figure 13. Comparison between slip, power, and drawbar pull (DP) force over time for two wheel configurations.**

### Overall Performance:

To analyze the overall performance of the wheels and gain a better understanding of the tradeoffs between wheel slip and power usage, we plotted these two metrics against each other and compared the results for each test (Figures 14 and 15). Instead of using the slip rates, as shown in Figures 8 and 9, we chose to instead plot the actual velocity of the robot. This velocity is a result of the wheel slip and was calculated by taking the slope of the actual distance traveled over time using linear regression. This metric was chosen over the slip rate because it is universally

positive and the numerical value itself is more directly relevant to the performance of the robot. Wheel slip is calculated by subtracting the actual distance traveled from the idealized distance traveled, so higher actual velocity is related to lower wheel slip rate.

Since the best wheel configuration will have both low slip (high actual velocity) and low power consumption, we examined the lower right quadrant of each graph. There is clearly no single wheel which performs the best in all conditions; for instance, while wheel #10 performed the best on all the circle tests, it performed poorly on the line tests. Many of the wheel configurations follow this trend of performing well on one type of test and badly on another. Based on the results from Figures 14 and 15, in order to design a wheel that will perform adequately in most or all situations, it is necessary to choose a wheel design that does not perform the best on any single test, but instead performs well holistically. Some wheel designs which seem to perform well overall are #5, #3, and #13.

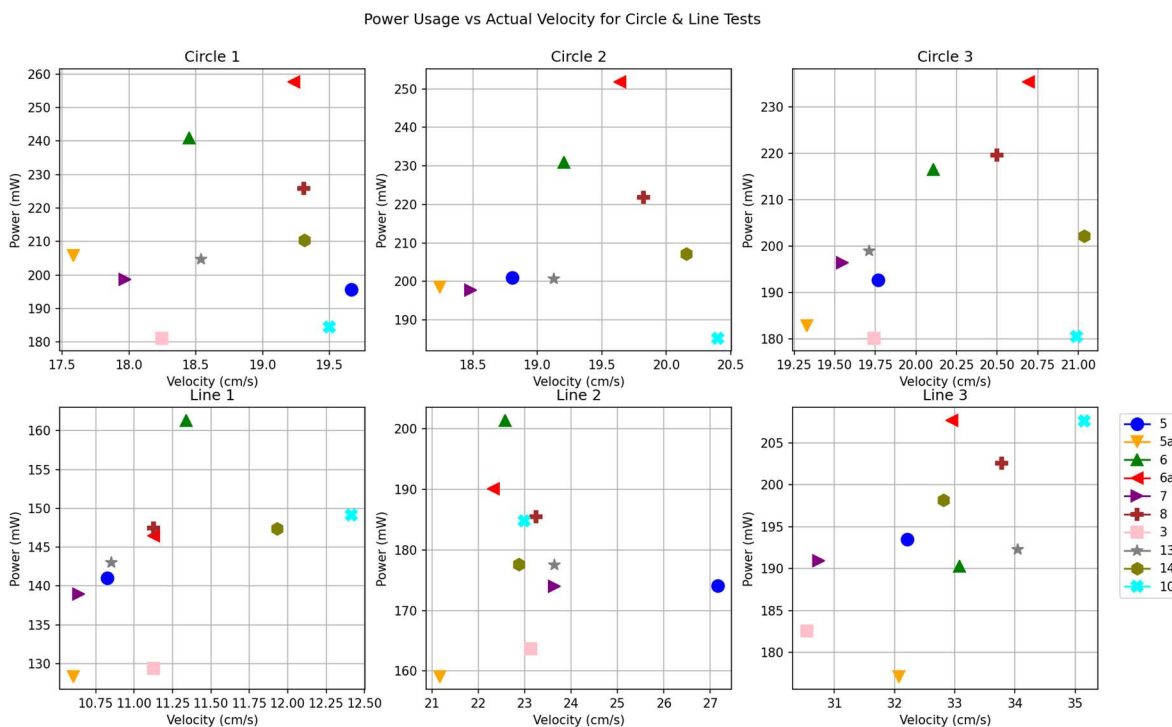


**Figure 14. Power usage vs actual velocity for circle and line driving tests.**

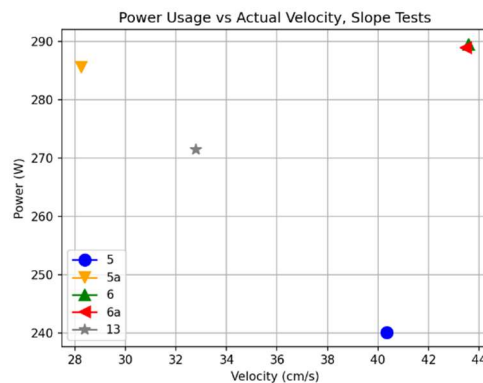


**Figure 15. Power usage vs actual velocity for slope test.**

## CONCLUSION

Although there was no single optimal wheel design that dominated the experimental results, there were numerous conclusions drawn from the data which will significantly impact the design of wheels for IPEX. First, there exists a tradeoff between wheel slip and power usage; wheels with taller square grousers will slip less than wheels with shorter, rounder grousers, but they will use more power. The wheel slip and power usage will need to be carefully balanced to address the needs of the mission. Next, the design of the cleats (“solid” vs “with holes”) did not seem to have a strong impact on either wheel slip or power usage. From a holistic design perspective, the cleats with holes are preferable since they will reduce the weight of the wheels, so it is useful to note that they do not perform noticeably worse than the wheels with the solid cleats. Finally, wheel performance changed depending on the test scenario. Further refinement of the wheel design for IPEX will need to be made as the concept of operations develops further, but a reasonable choice as a baseline wheel to perform adequately in most scenarios is wheel #5, which has short, rounded grousers. Additional research should focus on conducting more trials to ensure repeatability of the data, as well as further study into the effects of wheel design on performance specifically for skid-steer rovers.

## References

- Creager, C., Asnani, V., Oravec, H., Woodward, A. 2017. Drawbar Pull (DP) Procedures for Off-Road Vehicle Testing. NASA/TP—2017-219384. Glenn Research Center, Cleveland, OH.
- Ding, L., H. Gao, Z. Deng, K. Nagatani, K. Yoshida. 2011. “Experimental study and analysis on driving wheels’ performance for planetary exploration rovers moving in deformable soil.” *J. Terramechanics*. 48 (1), 27-45.
- Lawton, N. 2020. “Planetary rover wheel and lower leg structural design to reduce rock entanglements.” M.S. thesis, Luleå, Sweden: Luleå University of Technology.
- Mueller, R. P., Smith, J. D., Schuler, J. M., Nick, A. J., Gelino, N. J., Leucht, K. W., Townsend, I. I., & Dokos, A. G. 2016. Design of an Excavation Robot: Regolith Advanced Surface Systems Operations Robot (RASSOR) 2.0. Earth and Space 2016.
- Nagaoka, K., K. Sawada, K., Yoshida. 2020. “Shape effects of wheel grousers on traction performance on sandy terrain.” *J. Terramechanics*. 90, 23-30.
- Schuler, J., Nick, A., Leucht, K., Langton, A., Smith, D. 2022. ISRU Pilot Excavator: Bucket Drum Scaling Experimental Results. Earth and Space 2022.